THE UNIVERSITY OF MICHIGAN RESEARCH INSTITUTE
ANN ARBOR

TWO INTERFEROMETER-TYPE DIRECTION-FINDING SYSTEMS

Technical Report No. 89

Electronic Defense Group
Department of Electrical Engineering

By: S. I. Soclof

Approved by: H. W. Farris

Project 2899

TASK ORDER NO. EDG-10
CONTRACT NO. DA-36-039 sc-78283
SIGNAL CORPS, DEPARTMENT OF THE ARMY
DEPARTMENT OF ARMY PROJECT NO. 3-99-04-106

May 1959

TABLE OF CONTENTS

ABSTRACT

The analyses of two types of radio direction-finder are presented. These systems were investigated primarily with the VHF frequency range in mind. The analysis of the systems is presented for the purpose of indicating one way of instrumenting an interferometer system and to indicate a way of eliminating the ambiguities involved. Some discussion is given on the limitations of such systems. As with most direction finders in this frequency range and lower, the limitation on accuracy is a function of the environment and not solely dependent upon the instrumental accuracy of the equipment.

TWO INTERFEROMETER-TYPE DIRECTION-FINDING SYSTEMS

1. INTRODUCTION

This report will describe two proposed radio direction-finding systems based on the interferometer principle. From a theoretical standpoint the systems show certain advantages over other types of systems. However, it must be kept in mind that in a practical environment these advantages may not be realized because of the nature of operation of the systems. Both systems suffer in that they take samples of the wave front at only a few widely separated points and thus do not average over the wave front as would be desired.

2. THE "OAK-LEAF" DIRECTION FINDER

2.1 Principle of Operation

The first of the two systems investigated is called the "Oak-Leaf" DF because of the characteristic pattern produced by its antenna system. The system utilizes five antennas, as shown in Fig. 1.

Antennas 1 and 2 form a wide-spaced pair in terms of the wave length, λ. If the phase of the signal at antenna 2 is continually advanced with respect to that at antenna 1, a multilobed interference pattern is produced. A similar process obtains from the antenna pair 1 and 3 except that, since the spacing is slightly different, the resultant pattern will be rotated slightly in space, although similar in shape.

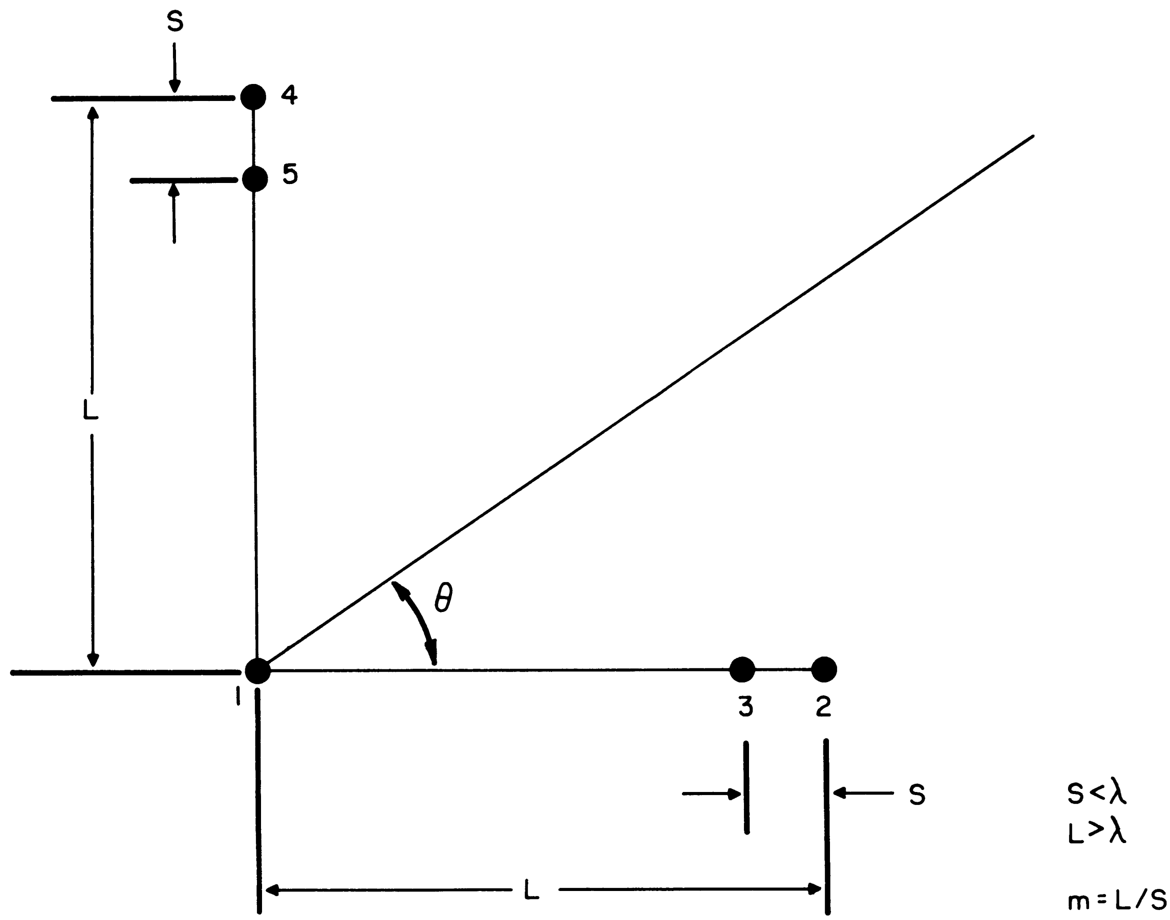

FIG.1 "OAK-LEAF" DF ANTENNA POSITIONING

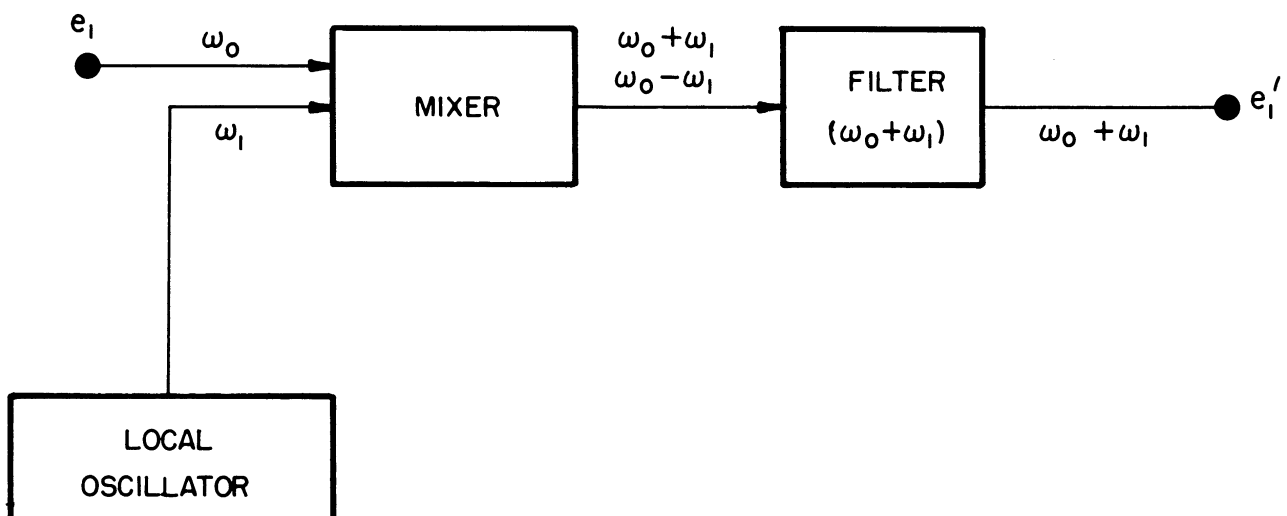

FIG. 2

Each pattern alone contains information as to the bearing of the transmitter but with ambiguities as represented by the multiplicity of lobes in the multilobed pattern. These ambiguities are resolved by a continuous rotation of one pattern with respect to the other so as to produce one major lobe which will indicate the direction of the target.

There remains, however, the reciprocal bearing ambiguity, which is resolved by using another antenna array, composed of antennas 1, 4, and 5, at right angles to the first.

2.2 System Analysis

The initial analysis concerns the antenna system comprised of antennas 1, 2, and 3; it is subsequently applied to the system of 1, 4, and 5.

Establish antenna 1 as the reference antenna and let the voltage at this antenna be represented by:

$$e_1 = A \cos \omega_0 t ,$$

where A involves system parameters involved with antenna 1.

Similarly,

$$e_3 = B \cos (\omega_0 t + \alpha) , \text{ and}$$

$$e_2 = C \cos (\omega_0 t + \beta) ,$$

where B and C represent system parameters peculiar to antennas 3 and 2, respectively, and

$$\alpha = \frac{2\pi}{\lambda_0} (L-S) \cos \Theta , \text{ and}$$

$$\beta = \frac{2\pi}{\lambda_0} (L) \cos \Theta .$$

Now, with reference to Fig. 2, if a locally generated signal at a frequency of $\omega_1/2\pi$ is mixed with e_1, the following is obtained:

$$e_{\omega_o} \times e_{\omega_1} = A \cos \omega_o t \times D \cos \omega_1 t$$
$$= \frac{AD}{2} \cos (\omega_o + \omega_1)t + \cos (\omega_o - \omega_1)t,$$

where $e_{\omega_1} = D \cos \omega_1 t$ is the oscillator voltage.
After filtering to retain only the $\omega_o + \omega_1$ term one obtains

$$e_1' = \frac{AD}{2}\cos (\omega_o + \omega_1)t \ .$$

Now, with reference to Fig. 3, a similar process is gone through, this time with e_1' and e_2.

$$e_1' \times e_2 = \left[\frac{AD}{2} \cos (\omega_o + \omega_1)t \right] \left[B \cos (\omega_o t + \alpha) \right]$$

$$= \frac{ADB}{4} \left[\cos (2\omega_o t + \omega_1 t + \alpha) + \cos (\alpha - \omega_1 t) \right]$$

After filtering to retain only the ω_1 term one obtains

$$e_2'' = \frac{ADB}{4} \cos (\alpha - \omega_1 t) \ .$$

Going through a similar process for e_3, one obtains

$$e_3'' = \frac{ADC}{4} \cos (\beta - \omega_1 t) \ .$$

Now introduce another locally generated signal given by

$$e_{\omega_2} = E \cos \omega_2 t \ .$$

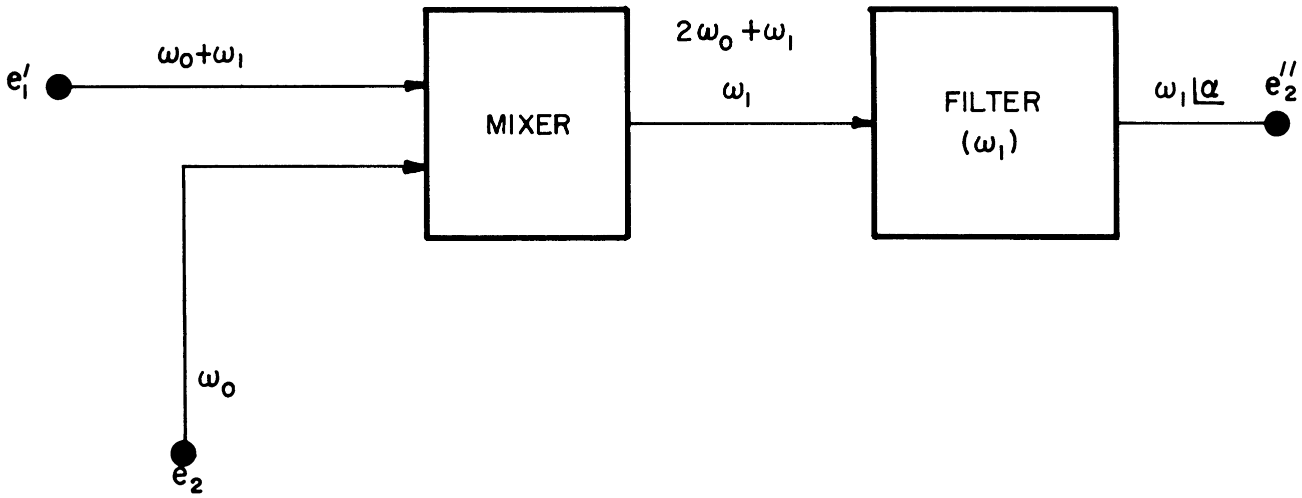

e_1'
$\omega_0+\omega_1$
MIXER
$2\omega_0+\omega_1$
ω_1
FILTER
(ω_1)
$\omega_1 \underline{|\alpha}$
e_2''
ω_0
e_2

FIG. 3

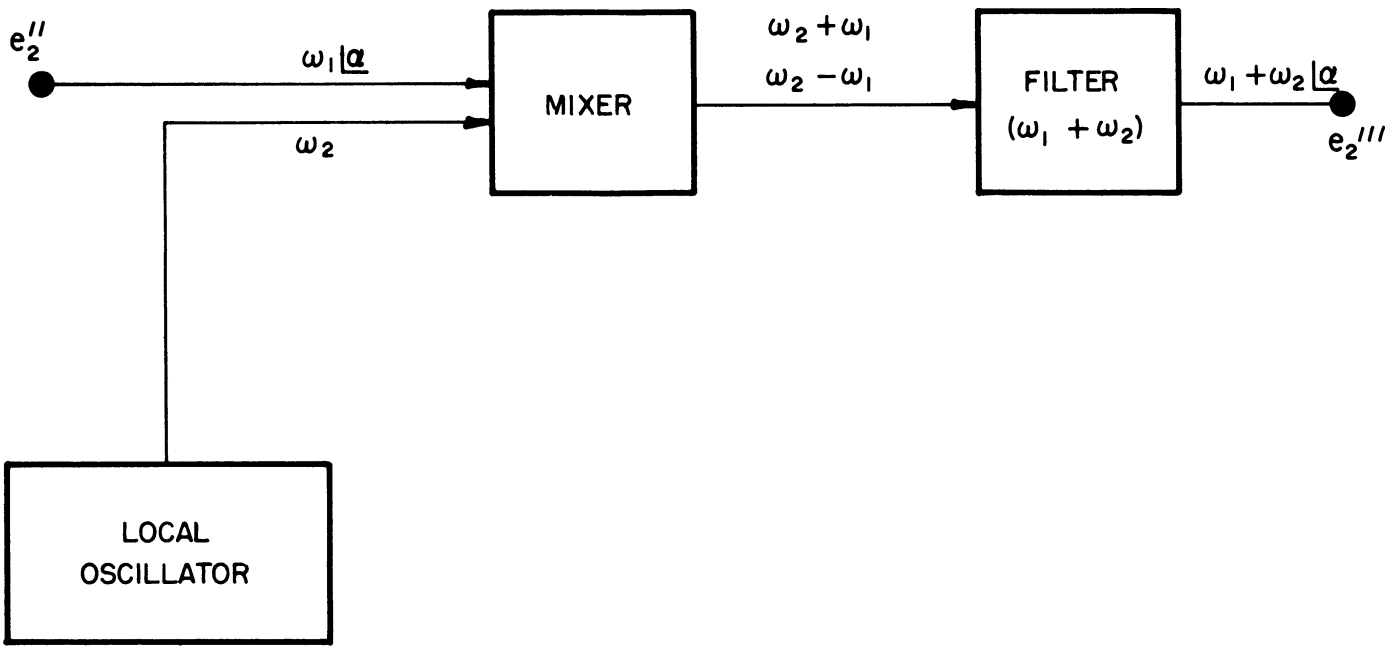

e_2''
$\omega_1 \underline{|\alpha}$
ω_2
MIXER
$\omega_2+\omega_1$
$\omega_2-\omega_1$
FILTER
$(\omega_1+\omega_2)$
$\omega_1+\omega_2 \underline{|\alpha}$
e_2'''
LOCAL
OSCILLATOR

FIG. 4

With reference to Fig. 4 it can be seen that one obtains

$$e_2'' \times e_{\omega_2} = \frac{ADB}{4} \cos (\alpha - \omega_1 t) \times E \cos (\omega_2 t)$$

$$= \frac{ADBE}{8} \left[\cos (\alpha + \omega_2 t - \omega_1 t) + \cos (\alpha - \omega_1 t - \omega_2 t)\right] .$$

After filtering to retain only the $\omega_2 + \omega_1$ term one obtains

$$e_2''' = \frac{ADBE}{8} \cos (\alpha - \omega_1 t - \omega_2 t) .$$

Now after the processing shown in Fig. 5, we find

$$e_2''' \times e_3'' = \frac{ABDE}{8} \cos \left[\alpha - (\omega_1 + \omega_2)t\right] \times \frac{ADC}{4} \cos (\beta - \omega_1 t) .$$

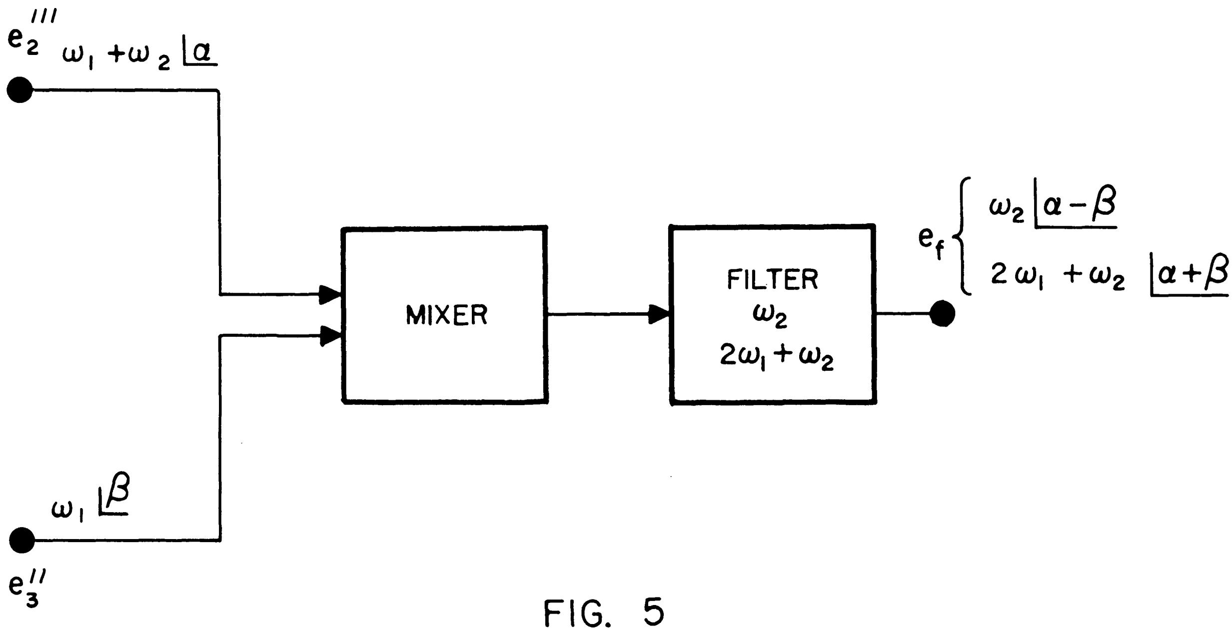

FIG. 5

$$e_f = \frac{A^2D^2BCE}{64}\left[\cos(\alpha + \beta - 2\omega_1 t - \omega_2 t) + \cos(\alpha - \beta + \omega_2 t)\right] .$$

By definition, $m = L/S$.

Now, since $\alpha = \frac{2\pi}{\lambda_o}(L-S)\cos\Theta$, and

$\beta = \frac{2\pi}{\lambda_o}(L)\cos\Theta$, we find that

$$\alpha + \beta = (2L-S)\frac{2\pi}{\lambda_o}\cos\Theta = (2Sm-S)\frac{2\pi}{\lambda_o}\cos\Theta = (2m-1)\frac{2\pi S}{\lambda_o}\cos\Theta \text{ , and}$$

$$\alpha - \beta = -\frac{2\pi S}{\lambda_o}\cos\Theta .$$

Now choose ω_1 and ω_2 such that $\frac{\omega_1}{\omega_2} = m - 1.$

$$\omega_1 = (m-1)\,\omega_2 ,$$

so: $$2\omega_1 + \omega_2 = 2m\omega_2 - 2\omega_2 + \omega_2 = 2m\omega_2 - \omega_2 = \omega_2(2m-1) .$$

Substituting all of this into the expression for e_f one obtains:

$$e_f = \frac{A^2D^2BCE}{64}\left\{\cos\left[(2m-1)\left(\frac{2\pi S}{\lambda_o}\right)\cos\Theta - (2m-1)\,\omega_2 t\right]\right.$$

$$\left. + \cos\left[\omega_2 t - \frac{2\pi S}{\lambda_o}\cos\Theta\right]\right\} \text{ , or}$$

$$e_f = \frac{A^2D^2BCE}{64}\left\{\cos\left[(2m-1)(\omega_2 t - \frac{2\pi S}{\lambda_o}\cos\Theta)\right] + \cos(\omega_2 t - \frac{2\pi S}{\lambda_o}\cos\Theta)\right\}.$$

Normalize e_f to prevent the resultant expression from ever becoming negative and call this $F(\Theta)$:

$$F(\Theta) = 2 + \cos\left[\omega_2 t - \frac{2\ S}{\lambda_o}\cos\Theta\right] + \cos\left[(2m-1)(\omega_2 t - \frac{2\pi S}{\lambda_o}\cos\Theta)\right] .$$

Let $\gamma = \frac{\omega_2}{2\pi}$. Now if $F(\Theta)$ is applied on a circular sweep of an oscilloscope being swept at a rate of $\gamma = \frac{\omega_2}{2\pi}$ revolutions per second one obtains a pattern given by:

$$F(\Theta) = 2 + \cos\left(\gamma - \frac{2\pi S}{\lambda_o}\cos\Theta\right) + \cos\left[(2m-1)\left(\gamma - \frac{2\pi S}{\lambda_o}\cos\Theta\right)\right] .$$

Figure 6 illustrates the particular case wherein $\Theta = 90^o$, but the same pattern will appear for any value of Θ except for a rotation around the origin.

Now, $F(\Theta)$ will have an absolute maximum when

$$\frac{2\pi S}{\lambda_o}\cos\Theta = \gamma .$$

From this one obtains $\cos\Theta$ as:

$$\cos\Theta = \gamma_{EW}\left(\frac{\lambda_o}{2\pi S}\right) .$$

Since $S < \frac{\lambda_o}{2}$ the only ambiguity involved in determining Θ will be in determining the correct algebraic sign to use. This is resolved by antennas 1, 4, and 5.

Going through the same signal processing as before, using antennas 1, 4, and 5 one obtains another value for γ, to be called γ_{NS}, from which one obtains $\sin\Theta$ by the relation:

$$\sin\Theta = \gamma_{NS}\left(\frac{\lambda_o}{2\pi S}\right) .$$

Having obtained γ_{NS} and γ_{EW} , one can now determine the angle of arrival, Θ, by constructing the triangle as shown in Fig. 7.

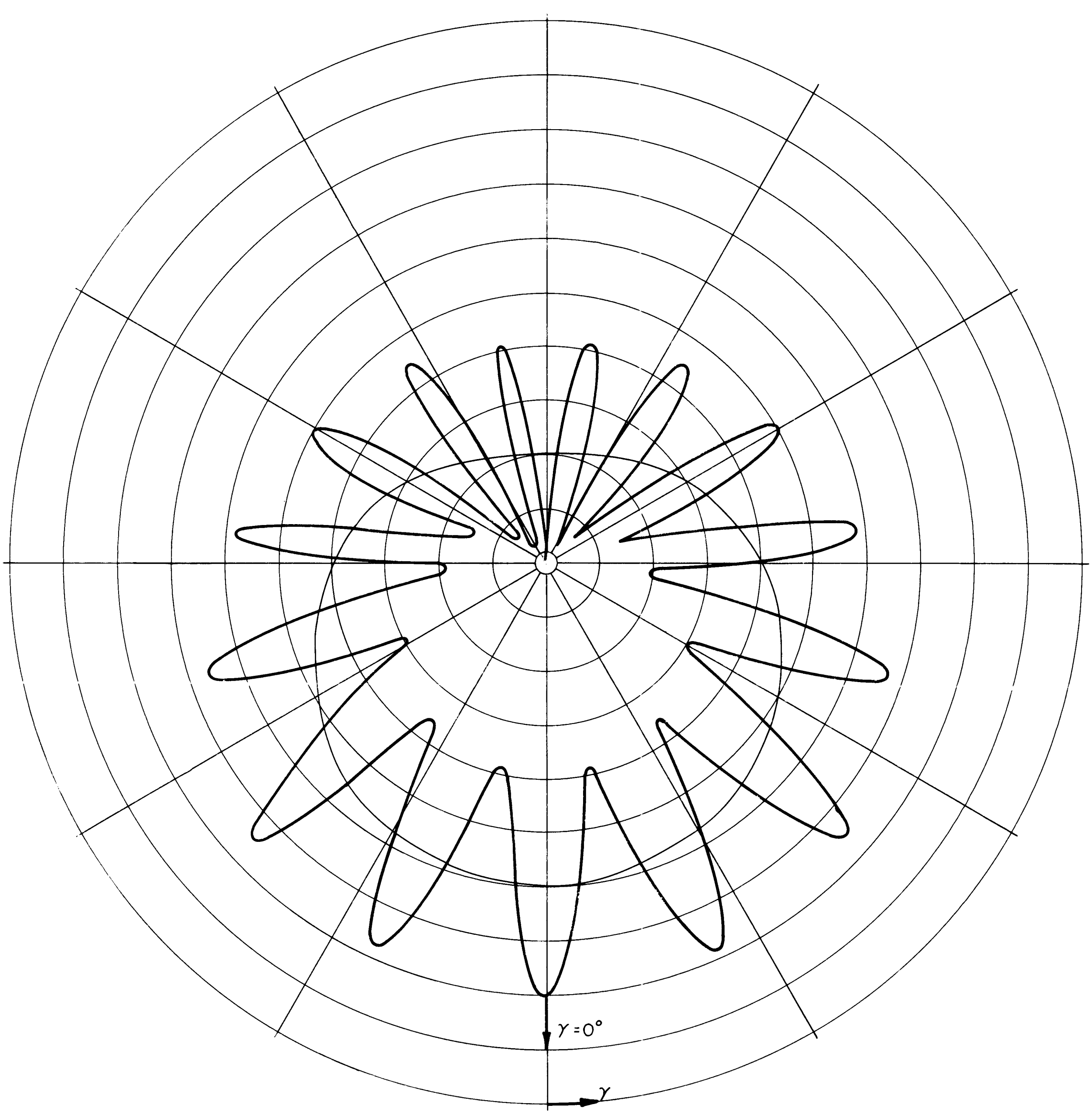

FIG.6 "OAK-LEAF" D F

$F(\theta) = 2 + \cos\gamma + \cos(15\gamma)$

$L/d = m = 8 \qquad \theta = 90°$

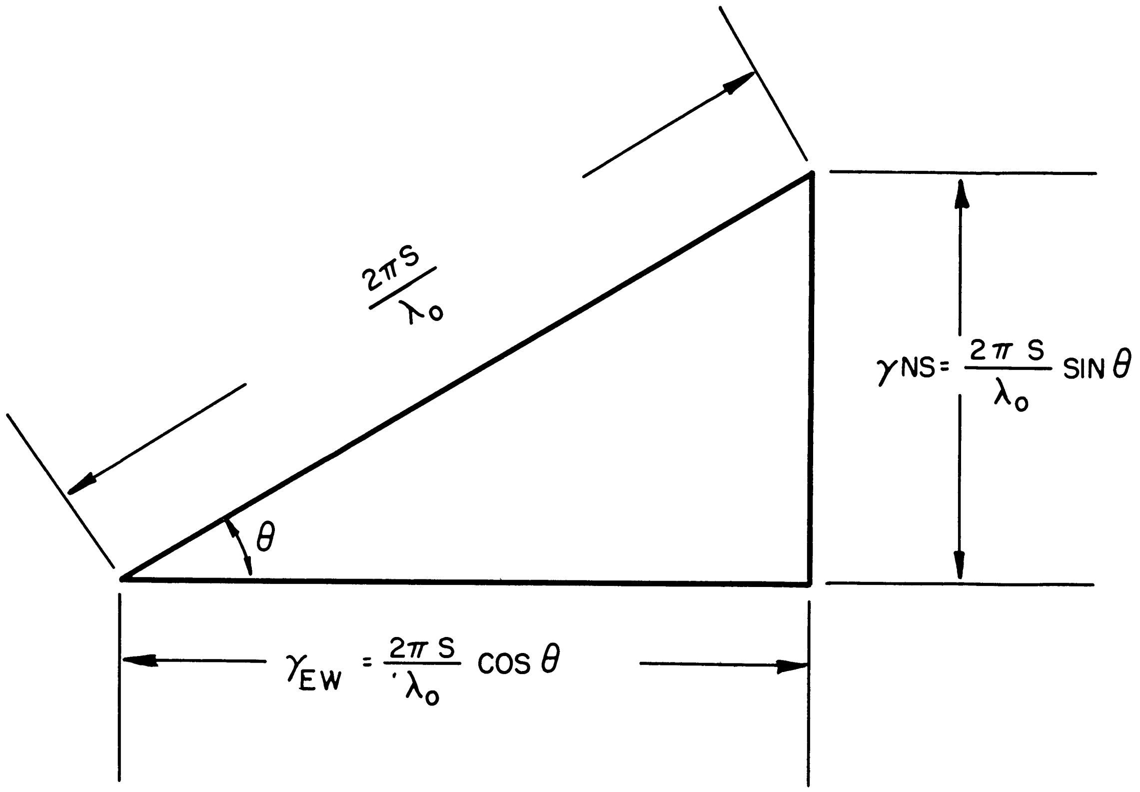

FIG.7 DETERMINATION OF θ

Note that the value of γ is independent of all the arbitrary amplitude constants, A, B, C, etc., so that the system will be relatively immune to amplitude unbalances.

Figure 8 shows a complete block diagram for the "Oak Leaf" DF.

3. THE "SPHERICAL WAVE-FRONT" SYSTEM

3.1 Principle of Operation

The "Spherical Wave-Front" system samples the incoming wave front at five points, one point serving as a reference point for the rest of the phases. Under ideal circumstances the wave propagating from a point source expands spherically, so that, by determining the shape of the wave front, one can determine not only the bearing of the target but also the range, thus determining the location or fix of the target.

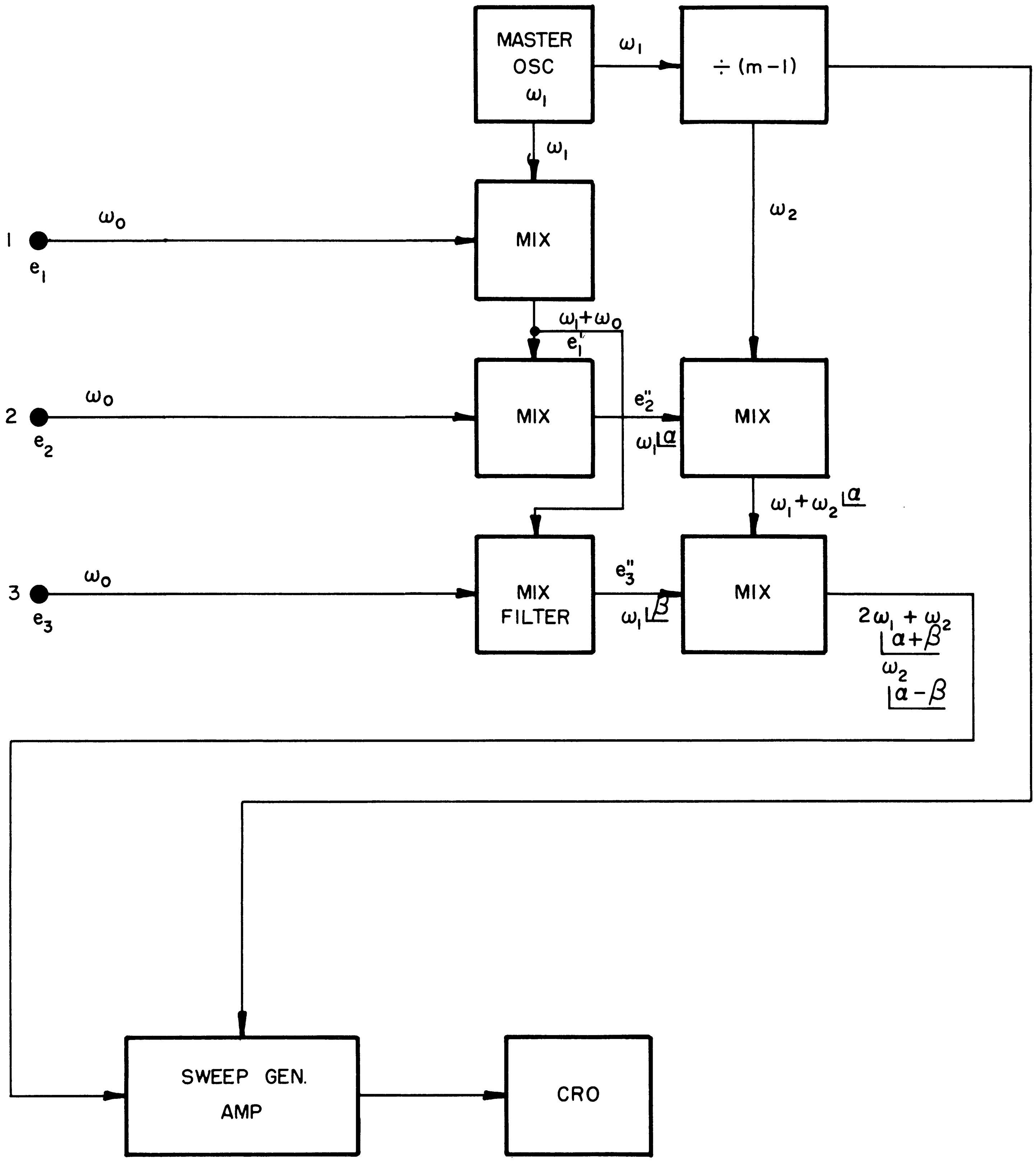

FIG.8 BLOCK DIAGRAM FOR "OAK-LEAF" D F

The determination of the shape of the wave front is done by comparing the relative phases of the incoming signal at each of the sampling points. Using these relative phases and certain approximations, one being that the array length, L, be much less than the distance to the transmitter, a fairly compact expression relating the bearing and range of the transmitter to the relative phases at each of the sampling points can be obtained.

In the proposed system, the signals from the sampling points are processed in such a way as to give a direct indication of the bearing and range.

3.2 System Analysis

First consider the signal processing necessary for the operation of the system and then briefly the circuits to perform these operations. The antenna positioning is as shown in Fig. 9. The target transmitter is at point P.

Now consider only antennas O and E as shown in Fig. 10. One finds that if $L \ll R$:

$$\alpha_{EO} = R - R_{PE} = \frac{L}{2} \cos \theta - \frac{L^2}{8R} \sin^2 \theta - \frac{L^3}{16R^2} \cos \theta \sin^2 \theta - \frac{L^4}{128R^3} (6 \cos^2 \theta - 1) + \ldots \quad .$$

Similarly:

$$\alpha_{WO} = R - R_{PW} = -\frac{L}{2} \cos \theta - \frac{L^2}{8R} \sin^2 \theta + \frac{\pi L^3}{16R^3} \cos \theta \sin^2 \theta - \frac{\pi L^4}{128R^3} (6 \cos^2 \theta - 1) + \ldots \quad .$$

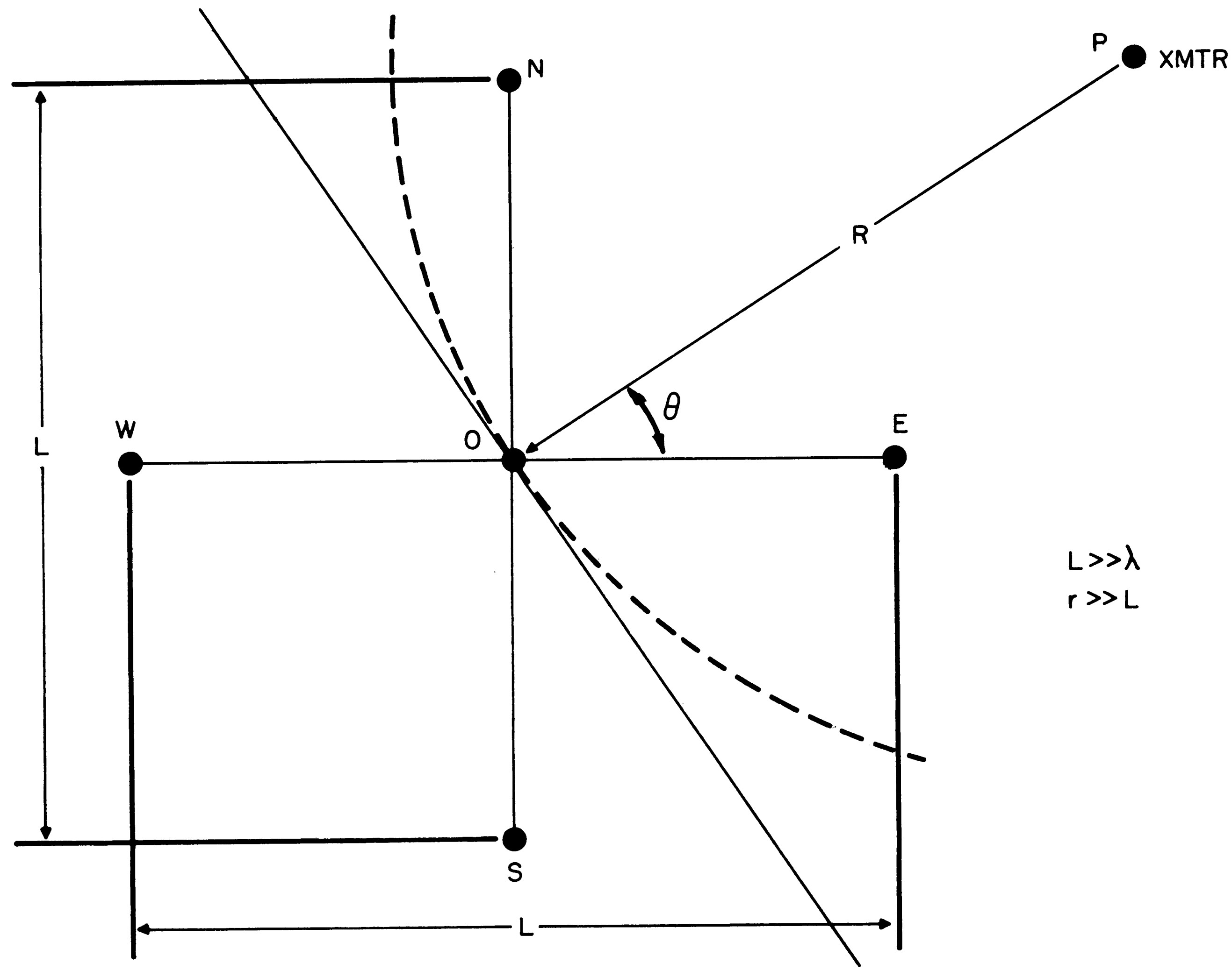

FIG. 9. ANTENNA POSITIONING FOR
"SPHERICAL WAVE-FRONT" SYSTEM

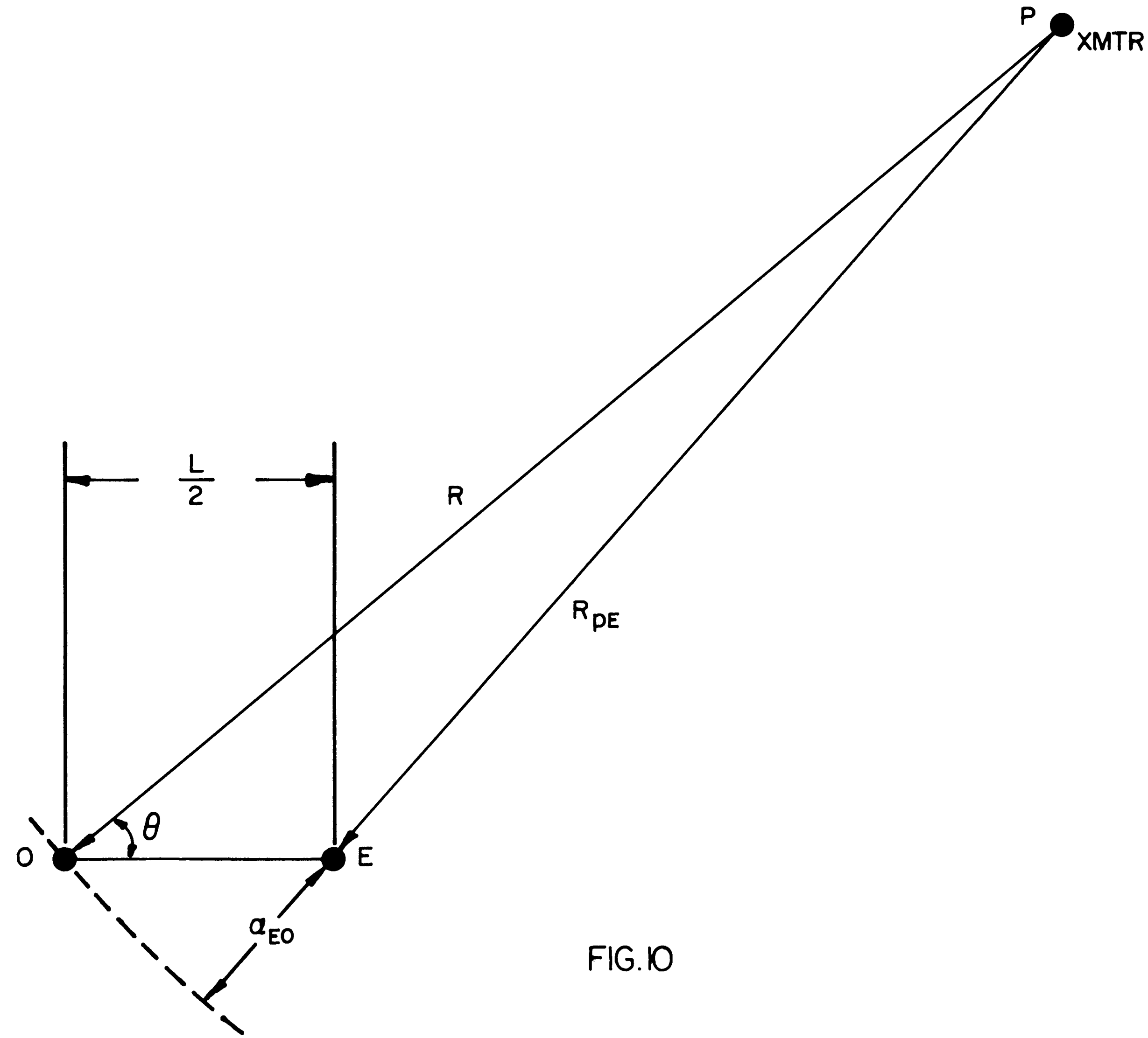

FIG.10

In terms of relative phase angles referred to antenna 0 as the reference point and dropping the higher order terms:

$$\varphi_{EO} = \frac{2\pi}{\lambda} \alpha_{EO} = \frac{\pi L \cos \theta}{\lambda} - \frac{\pi L^2 \sin^2 \theta}{4R\lambda} + \ldots$$

$$\varphi_{WO} = \frac{2\pi}{\lambda} \alpha_{WO} = - \frac{\pi L \cos \theta}{\lambda} - \frac{\pi L^2 \sin^2 \theta}{4R\lambda} + \ldots$$

and similarly:

$$\varphi_{NO} = \frac{\pi L \sin \theta}{\lambda} - \frac{\pi L^2}{4R\lambda} \cos^2 \theta + \ldots$$

$$\varphi_{SO} = - \frac{\pi L \sin \theta}{\lambda} - \frac{\pi L^2}{4R\lambda} \cos^2 \theta + \ldots$$

Now add φ_{EO} and φ_{WO} to obtain φ_{EW}:

$$\varphi_{EW} = \varphi_{EO} + \varphi_{WO} = - \frac{\pi L^2}{2R\lambda} \sin^2 \theta + \ldots$$

Similarly for φ_{NS}:

$$\varphi_{NS} = \varphi_{NO} + \varphi_{SO} = - \frac{\pi L^2}{2R\lambda} \cos^2 \theta + \ldots$$

Next take the sum of φ_{EW} and φ_{NS} to be called φ_{EWNS}:

$$\varphi_{EWNS} = \varphi_{EW} + \varphi_{NS} = - \frac{\pi L^2}{2R\lambda} \sin^2 \theta + \cos^2 \theta + \ldots$$

$$\varphi_{EWNS} = - \frac{\pi L^2}{2R\lambda} + \ldots$$

Solving this for R one obtains:

$$R \doteq - \frac{\pi L^2}{2\lambda\varphi_{EWNS}}$$

Now take the quotent of φ_{EW} and φ_{EWNS}:

$$\frac{\varphi_{EW}}{\varphi_{EWNS}} \doteq \frac{-\dfrac{\pi L^2 \sin^2 \theta}{2R\lambda}}{-\dfrac{\pi L^2}{2R\lambda}}$$

Solving this for $\sin^2 \theta$ one obtains:

$$\sin^2 \theta \doteq \frac{\varphi_{EW}}{\varphi_{EWNS}}$$

Similarly:

$$\cos^2 \theta \doteq \frac{\varphi_{NS}}{\varphi_{EWNS}}$$

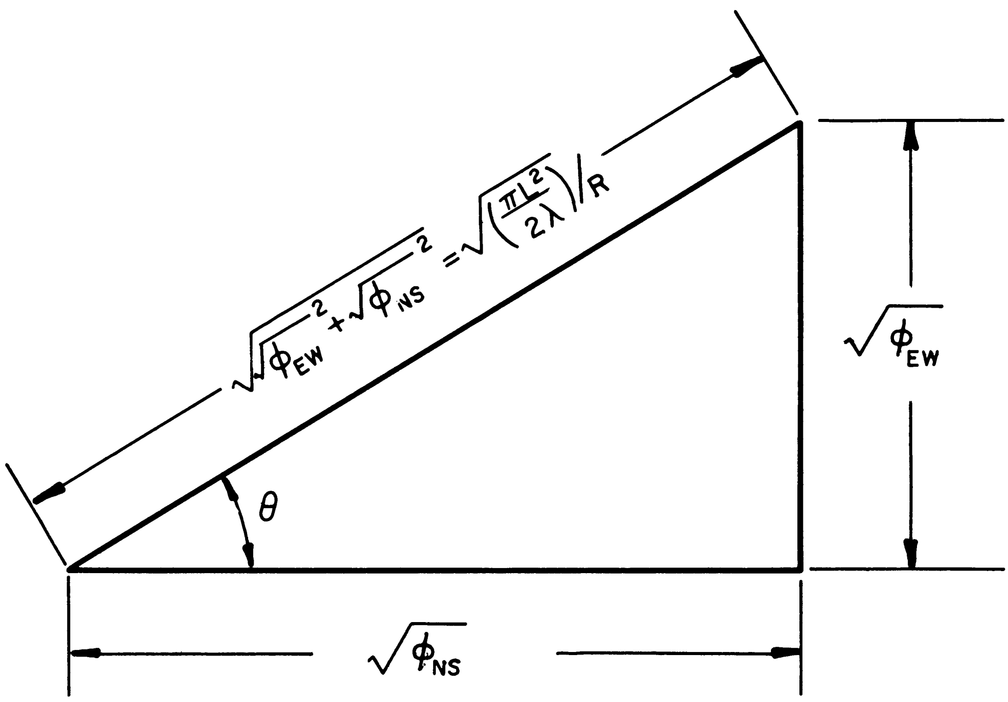

FIG. 11 DETERMINATION OF RANGE AND BEARING

Since

$$\sin \Theta \doteq \frac{\sqrt{\varphi_{EW}}}{\sqrt{(\sqrt{\varphi_{EW}})^2 + (\sqrt{\varphi_{NS}})^2}}$$

and

$$\cos \Theta \doteq \frac{\sqrt{\varphi_{NS}}}{\sqrt{(\sqrt{\varphi_{EW}})^2 + (\sqrt{\varphi_{NS}})^2}}$$

we can construct the diagram shown in Fig. 11.

3.3 Possible Method of Instrumentation

φ_{EO} is the phase angle by which the signal at antenna E leads that at antenna O. φ_{WO} is likewise the phase angle by which the signal at antenna W leads that at reference antenna O. Let the voltage e_E, e_W, and e_O be respectively:

$$e_E = E \sin(\omega_o t + \varphi_{EO}),$$

$$e_W = W \sin(\omega_o t + \varphi_{WO}), \text{ and}$$

$$e_O = A \sin(\omega_o t),$$

where E, W, and A are arbitrary constants involving the system parameters.

First, by the processing shown in Fig. 12, one takes the product e_E and e_W to be called e_{EW}:

$$e_E \times e_W = E \sin(\omega_o t + \varphi_{EO}) \times W \sin(\omega_o t + \varphi_{WO})$$

$$= \frac{EW}{2}\left[\cos(\varphi_{EO} - \varphi_{WO}) - \cos(2\omega_o t + \varphi_{EO} + \varphi_{WO})\right] .$$

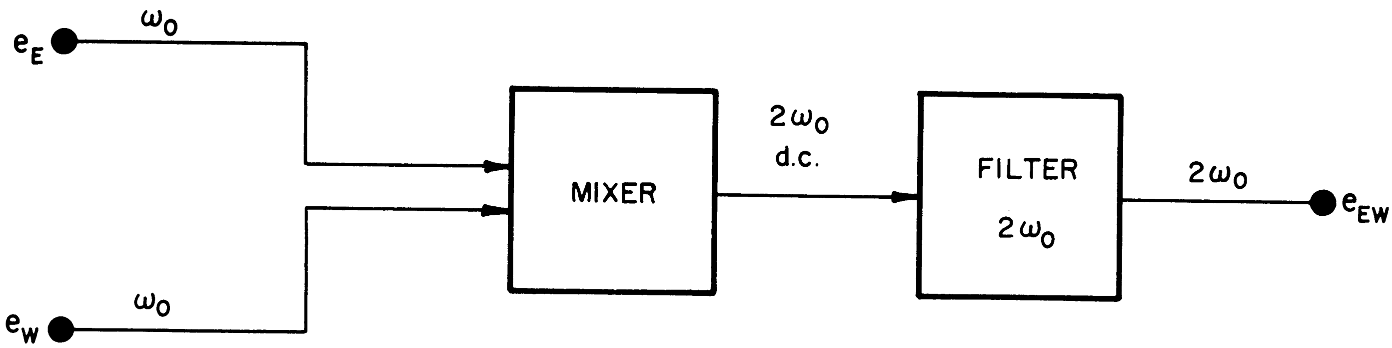

FIG. 12

After filtering to retain only the $2\omega_o$ term one has:

$$e_{EW} = -\frac{EW}{2}\cos(2\omega_o t + \varphi_{EO} + \varphi_{WO})$$

$$= -\frac{EW}{2}\cos(2\omega_o t + \varphi_{EW}) .$$

Next one takes a locally generated signal at a radian frequency of $\omega_o + \beta$ to be called e_B:

$$e_B = B \sin(\omega_o + \beta)t .$$

By processing shown in Fig. 13 one obtains the following:

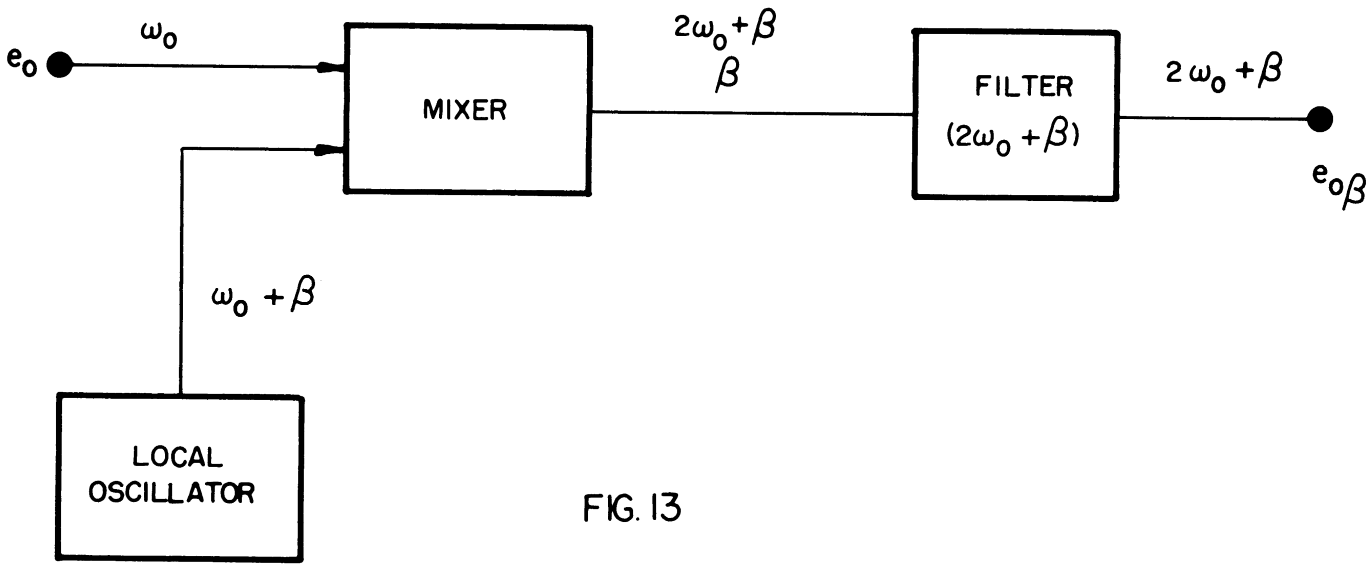

FIG. 13

$$e_O \times e_B = A \sin \omega_o t \times B \sin (\omega_o + \beta)t$$

$$= \frac{AB}{2} \cos \beta t - \cos (2\omega_o + \beta)t \quad .$$

Now, by filtering, one takes only the $2\omega_o + \beta$ component of e_{OB}:

$$e_{OB} = - \frac{AB}{2} \cos (2\omega_o + \beta)t \quad .$$

Next, as shown in Fig. 14, one takes the product of e_{EW} and e_{OB} to be called e_{EWO}:

$$e_{EW} \times e_{OB} = - \frac{EW}{2} \cos (2\omega_o t + \varphi_{EW}) \times - \frac{AB}{2} \cos (2\omega_o t + \beta t)$$

$$= \frac{EWAB}{8} \left[\cos (\beta t - \varphi_{EW}) + \cos (4\omega_o t + \beta t + \varphi_{EW})\right] \quad .$$

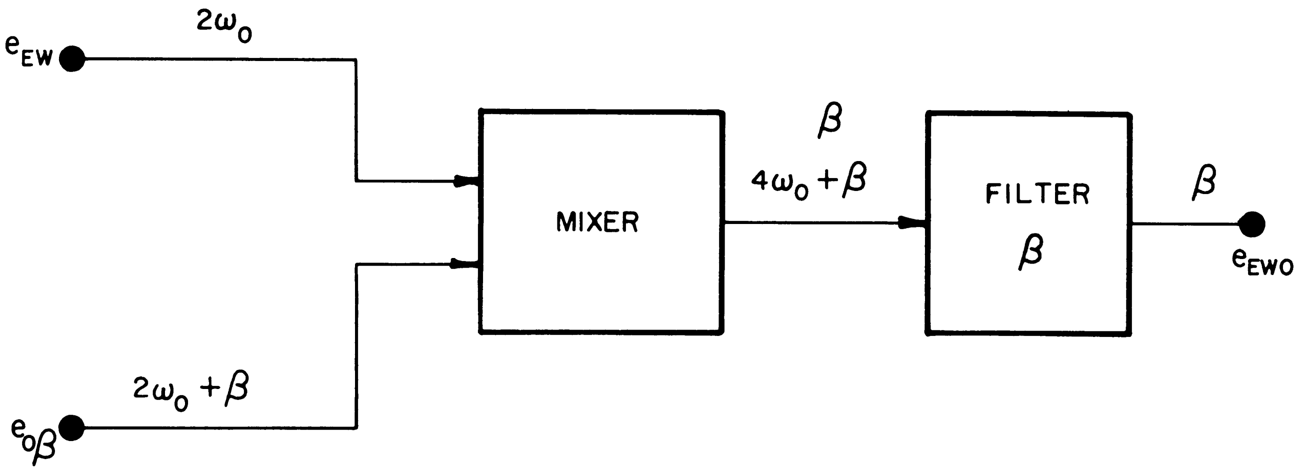

FIG. 14

After retaining only the β term:

$$e_{EWO} = \frac{EWAB}{8} \cos\ (\beta t - \varphi_{EW}) \quad .$$

In a similar manner, the signals from antennas N and S together with that from antenna O could be processed to give:

$$e_{NSO} = \frac{NSAB}{8} \cos\ (\beta t - \varphi_{NS}) \quad .$$

The next step is the derivation of a voltage proportional to $\sqrt{\varphi_{EW}}$ and $\sqrt{\varphi_{NS}}$.

Consider Fig. 15.

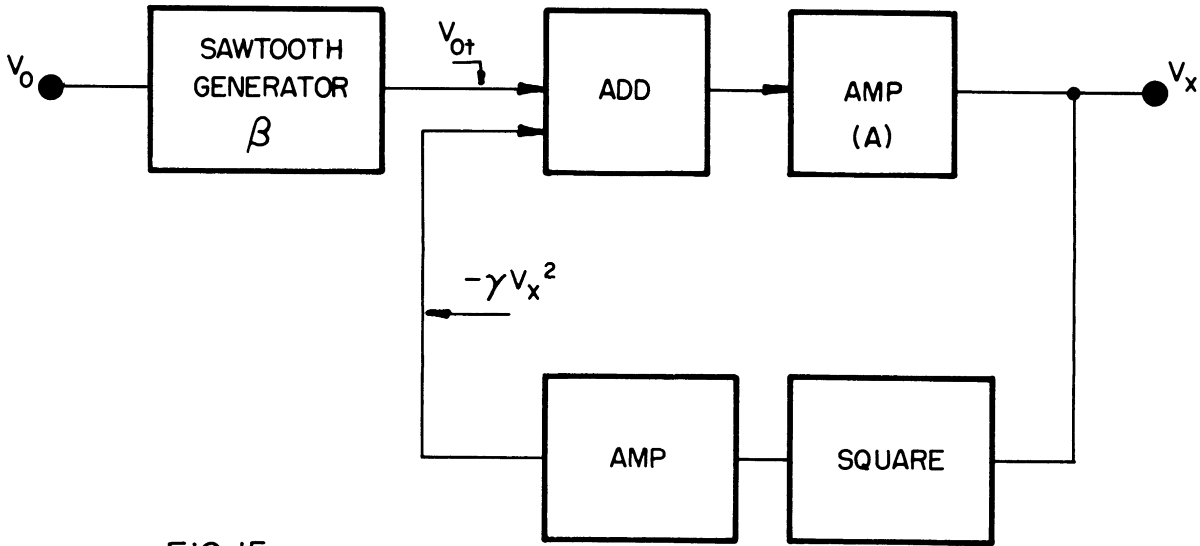

FIG. 15

The output voltage, V_x, is given by:

$$V_x = -\frac{1}{2A\gamma} + \sqrt{\frac{V_o t}{\gamma}\left(1 + \frac{1}{4A^2\gamma V_o t}\right)} \quad .$$

For values of A, γ, and t, such that

$$\sqrt{V_o t} \gg -\frac{1}{2A\sqrt{\gamma}} \quad \text{and} \quad 4A^2\gamma V_o t \gg 1 \; ,$$

V_x can be represented approximately by:

$$V_x \doteq \sqrt{\frac{V_o t}{\gamma}} \qquad \sqrt{t}$$

Now one has a voltage, V_x, which is proportional to the square root of time, t.

Now send e_{EWO} and e_{OB} through the wave shaping processing shown in Fig. 16.

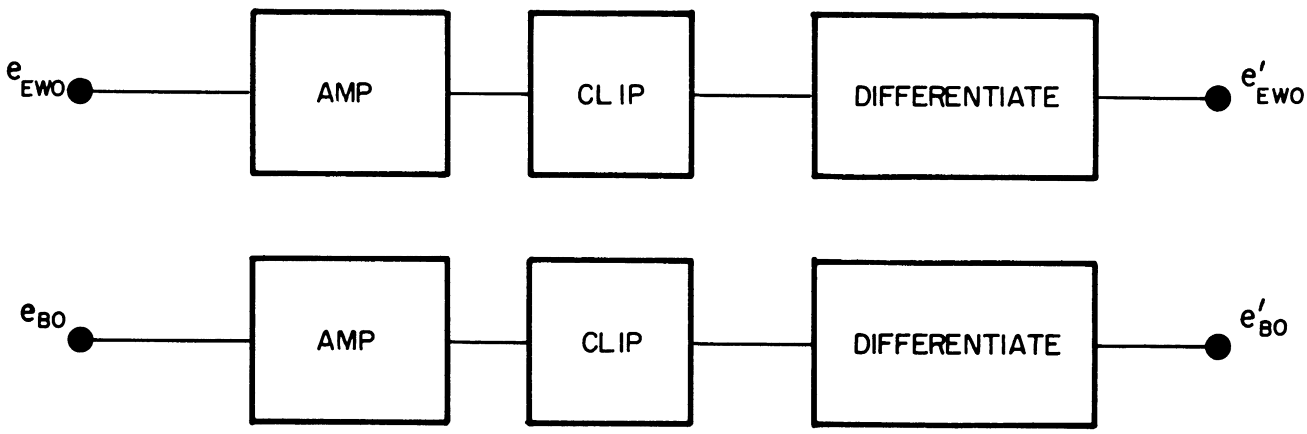

FIG. 16

The output e'_{BO} is a series of sharp pulses with a recurrence interval of time, $T_o = \frac{2\pi}{\beta}$, but lags the pulses of e_{BO} by a time, $T = \frac{\Phi_{EW}}{\beta}$, as shown in Fig. 17.

Now if one takes the voltage V_x, which also has a fundamental period of $T_o = \frac{2\pi}{\beta}$, and considers its value at t = T, one obtains a voltage V_{EW} proportional to $\sqrt{\varphi_{EW}}$. Similarly, $V_{NS} \sim \sqrt{\varphi_{NS}}$.

Now, if V_{EW} is applied to the y-axis of an oscilloscope, and V_{NS} is applied to the x-axis, a triangle can be constructed as shown in Fig. 18. However, there still remains some quadrantal ambiguity. This ambiguity can be resolved by some additional instrumentation since this information is present in the unprocessed signals.

A complete block diagram of the system is shown in Fig. 19.

4. PERFORMANCE OF INTERFEROMETER DF SYSTEMS IN TERMS OF ACTUAL PROPAGATION CONDITIONS

Each of the systems discussed determines the bearing of a transmitter by sampling the wave front at a few widely separated points.

In the "Oak-Leaf" DF, the bearing is determined from these samples by comparing the relative phases at each of the sampling points; from these relative phases an imaginary phase front can be drawn which under ideal propagation conditions, will coincide with the actual phase front. The bearing is determined from the phase front by a perpendicular to the phase front at the DF site.

The "Spherical Wave-Front" system proceeds one step further than the previous system: not only are the relative phases compared, but the differences in relative phases are compared in order to obtain as an end result an imaginary phase front as before represented, this time, by the arc of a circle. Again, under ideal propagation conditions, the imaginary

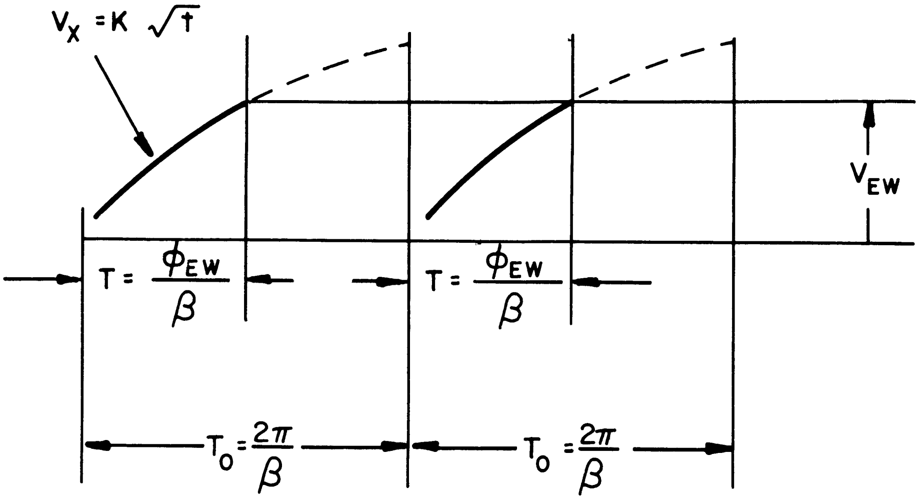

FIG. 17

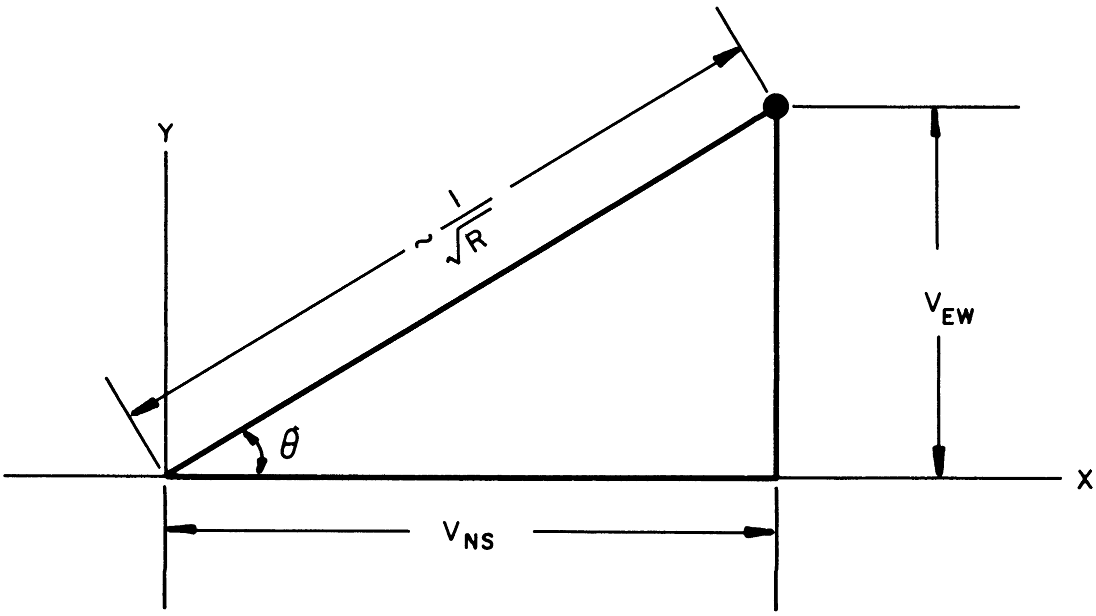

FIG. 18. PRESENTATION OF RANGE AND BEARING INFORMATION ON CRO

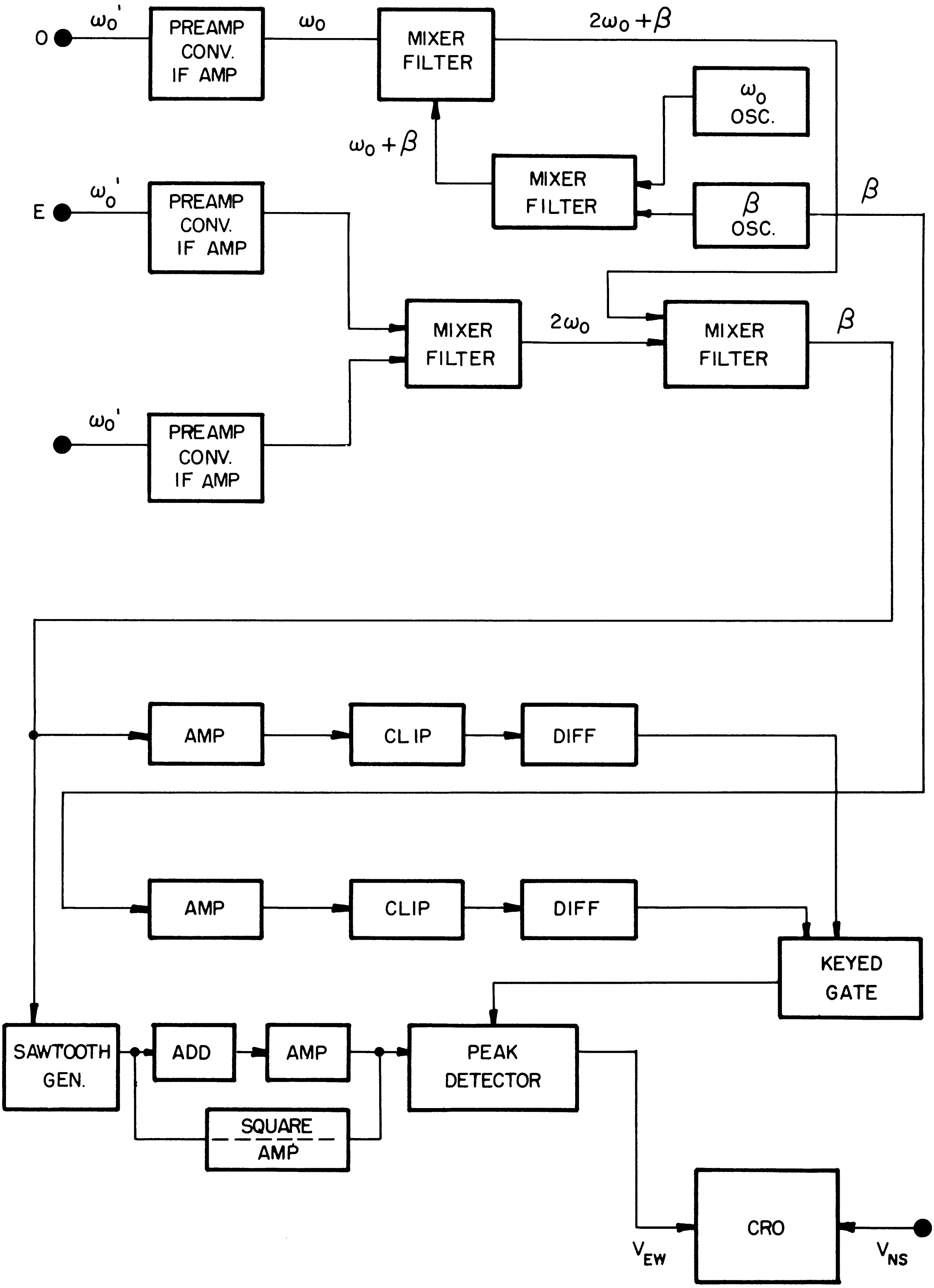

FIG.19 BLOCK DIAGRAM OF SPHERICAL WAVE-FRONT SYSTEM

phase front will coincide with the actual phase front. In this system the bearing and also the range are determined by locating the center of the circular arc.

In either system the fundamental difficulty is the same. Each system samples the wave front at only a few widely separated points and in no way attempts to determine the average wave front between these points. The "Spherical Wave-Front" system is a bit worse in this respect. Not only does it compare the relative phases at the several points and then take the differences of these phases as does the "Oak-Leaf" DF, but it goes one step further and takes differences of the differences of the relative phases, thus leaving the system open to the possibility of very serious errors. Perhaps this may be seen more clearly by referring to Fig. 20. In the "Oak-Leaf" DF system the bearing of the transmitter is determined by essentially comparing length P1 with length P0 to derive a difference length ΔL = P0-P1, which is determined in terms of phase angles. Since ΔL will be a very small quantity as compared to P0 or P1 it can be seen that a very small difference in two large quantities is being taken, which will lead to serious errors when actual propagation conditions cause the average velocity of wave propagation over path P1 to differ from that over path P0.

Looking at Fig. 21, which represents the conditions involved in the "Spherical Wave-Front" system, it is seen that in this system that distance P0 is compared to PE and also to distance PW to obtain difference lengths ΔEO = P0-PE and ΔWO = P0-PW, respectively. Then ΔEO is compared to ΔWO to obtain the second difference, $\Delta EW = \Delta EO - \Delta WO$, which is expressed in terms of phase angles, all with respect to the phase of the signal at antenna 0.

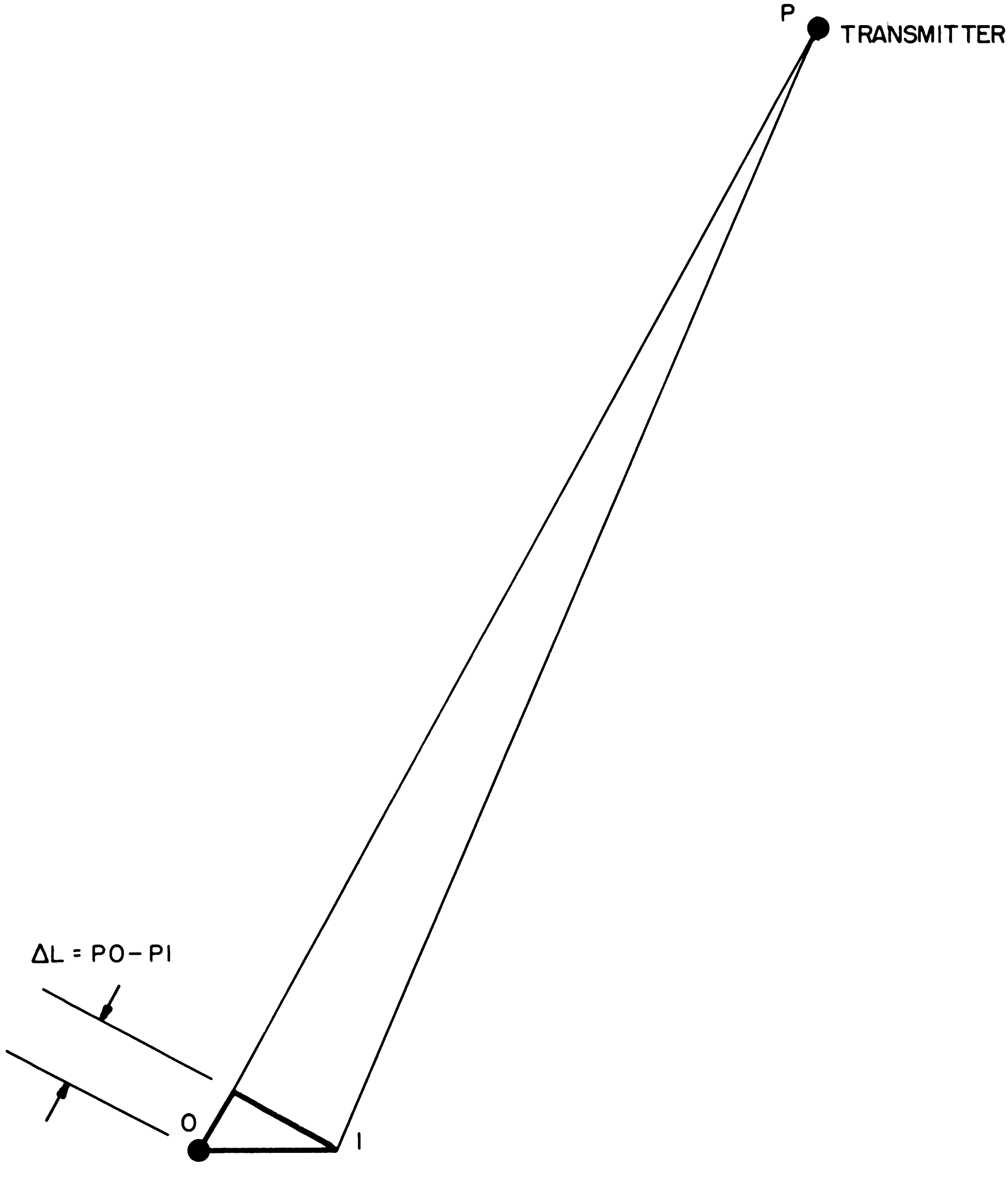

FIG. 20

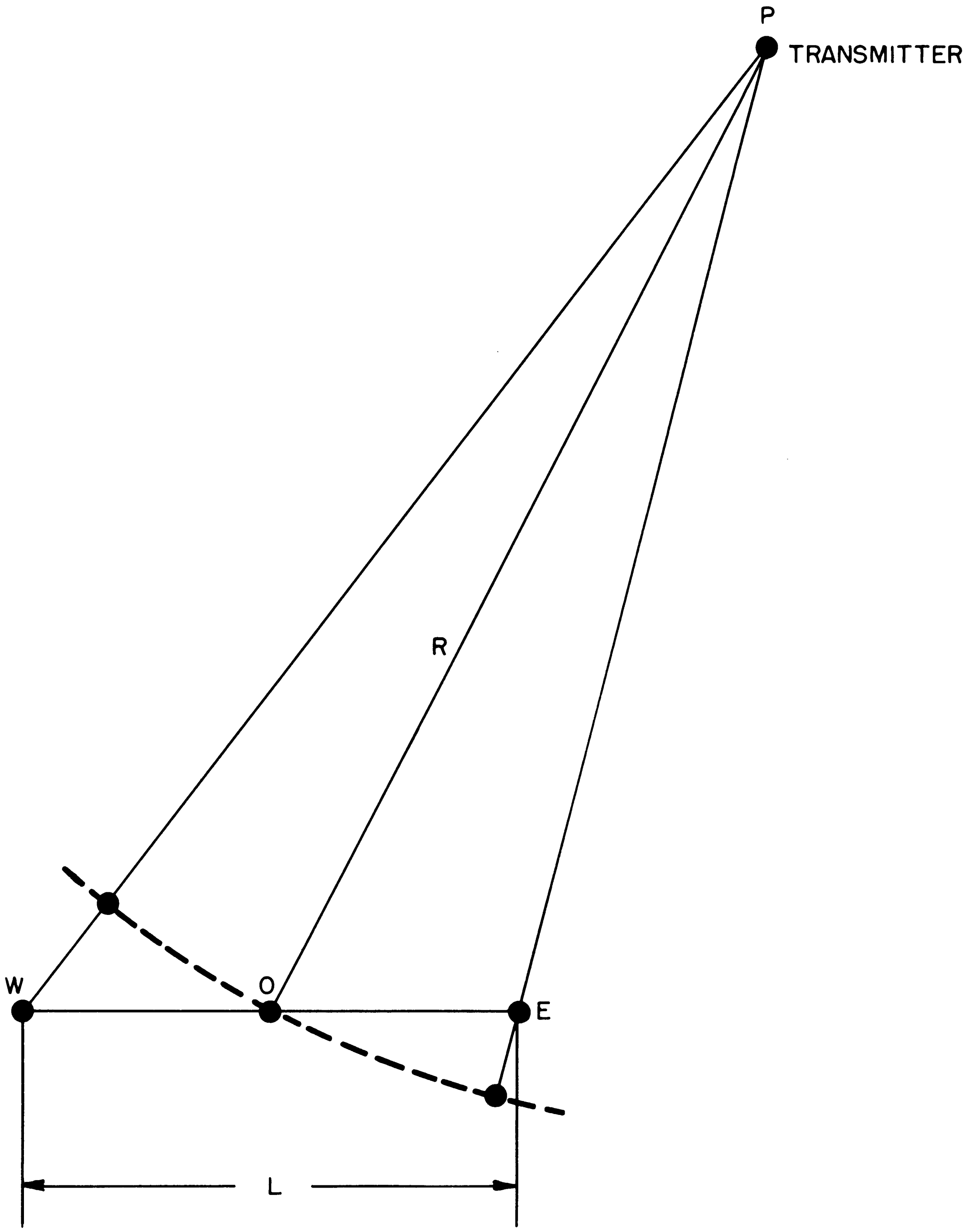

FIG. 21

Since the array length L is very small compared to the distance R, it can be seen that only a very small difference in the average velocity of wave propagation over the three paths, PE, PO, and PW, can cause extremely large errors in the bearing and range. Also, since the resultant phase angle to be measured is likely to be extremely small except in the special case of the transmitter being very close to the direction-finding site, the instrumental errors are likely to be very large, if not the prime determining factor in the practicality of the system.

5. CONCLUSIONS

The analysis section of this report presents two methods of instrumenting two interferometer DF systems. In order to determine the usability of these systems in a real situation, one should make an error analysis using perturbation data for the particular case involved. It appears that as one increases the aperture in the manner of an interferometer system without increasing the number of sampling points that the system may be more susceptible to environmental errors than would ordinarily be the case, and, as is pointed out in the report, more sample points in the space are needed.

DISTRIBUTION LIST

Copy No.	
1-2	Commanding Officer, U. S. Army Signal Research and Development Laboratory, Fort Monmouth, New Jersey, ATTN: Senior Scientist, Countermeasures Division
3	Commanding General, U. S. Army Electronic Proving Ground, Fort Huachuca, Arizona, ATTN: Director, Electronic Warfare Department
4	Chief, Research and Development Division, Office of the Chief Signal Officer, Department of the Army, Washington 25, D.C. ATTN: SIGEB
5	Chief, Plans and Operations Division, Office of the Chief Signal Officer, Washington 25, D.C., ATTN: SIGEW
6	Commanding Officer, Signal Corps Electronics Research Unit, 9560th USASRU, P.O. Box 205, Mountain View, California
7	U.S. Atomic Energy Commission, 1901 Constitution Avenue, N.W., Washington 25, D.C., ATTN: Chief Librarian
8	Director, Central Intelligency Agency, 2430 E. Street, N.W., Washington 25, D.C., ATTN: OCD
9	Signal Corps Liaison Officer, Lincoln Laboratory, Box 73, Lexington 73, Massachusetts, ATTN: Col. Clinton W. Janes
10-19	Commander, Armed Services Technical Information Agency, Arlington Hall Station, Arlington 12, Virginia
20	Commander, Air Research & Development Command, Andrews Air Force Base, Washington 25, D.C., ATTN: RDTC
21	Directorate of Research & Development, USAF, Washington 25, D.C., ATTN: Chief, Electronic Division
22-23	Commander, Wright Air Development Center, Wright-Patterson Air Force Base, Ohio, ATTN: WCOSI-3
24	Commander, Wright Air Development Center, Wright-Patterson Air Force Base, Ohio, ATTN: WCIGL-7
25	Commander, Air Force Cambridge Research Center, L.G. Hanscom Field, Bedford, Massachusetts, ATTN: CROTLR-2

Copy No.	
26	Commander, Rome Air Development Center, Griffiss Air Force Base, New York, ATTN: RCSSLD
27	Commander, Air Proving Ground Center, ATTN: Adj/Technical Report Branch, Eglin Air Force Base, Florida
28	Commander, Special Weapons Center, Kirtland Air Force Base, Albuquerque, New Mexico
29	Chief, Bureau of Ordnance, Code ReO-1, Department of the Navy, Washington 25, D.C.
30	Chief of Naval Operations EW Systems Branch, OP-347, Department of the Navy, Washington 25, D.C.
31	Chief, Bureau of Ships, Code 840, Department of the Navy, Washington 25, D.C.
32	Chief, Bureau of Ships, Code 843, Department of the Navy, Washington 25, D.C.
33	Chief, Bureau of Aeronautics, Code EL-8, Department of the Navy, Washington 25, D.C.
34	Commander, Naval Ordnance Test Station, Inyokern China Lake, California, ATTN: Test Director-Code 30
35	Commander, Naval Air Missile Test Center, Point Mugu, California, ATTN: Code 366
36	Director, Naval Research Laboratory, Countermeasures Branch, Code 5430, Washington 25, D.C.
37	Director, Naval Research Laboratory, Washington 25, D.C., ATTN: Code 2021
38	Director, Air University Library, Maxwell Air Force Base, Alabama, ATTN: CR-4987
39	Commanding Officer-Director, U.S. Naval Electronic Laboratory, San Diego 52, California
40	Office of the Chief of Ordnance, Department of the Army, Washington 25, D.C., ATTN: ORDTU
41	Chief, West Coast Office, U.S. Army Signal Research and Development Laboratory, Bldg. 6, 75 S. Grand Avenue, Pasadena 2, California

DISTRIBUTION LIST (Cont'd)

Copy No.	
42	Commanding Officer, U.S. Naval Ordnance Laboratory, Silver Spring 19, Maryland
43-44	Chief, U.S. Army Security Agency, Arlington Hall Station, Arlington 12, Virginia, ATTN: GAS-24L
45	President, U.S. Army Defense Board, Headquarters, Fort Bliss, Texas
46	President, U.S. Army Airborne and Electronics Board, Fort Bragg, North Carolina
47	U.S. Army Antiaircraft Artillery and Guided Missile School, Fort Bliss, Texas, ATTN: E&E Dept.
48	Commander, USAF Security Service, San Antonio, Texas, ATTN: CLR
49	Chief of Naval Research, Department of the Navy, Washington 25, D.C., ATTN: Code 931
50	Commanding Officer, U.S. Army Security Agency, Operations Center, Fort Huachuca, Arizona
51	President, U.S. Army Security Agency Board, Arlington Hall Station, Arlington 12, Virginia
52	Operations Research Office, Johns Hopkins University, 6935 Arlington Road, Bethesda 14, Maryland, ATTN: U.S. Army Liaison Officer
53	Commanding Officer, U.S. Army Signal Research & Development Laboratory, Fort Monmouth, New Jersey, ATTN: U.S. Marine Corps Liaison Office, Code AO-4C.
54	Commanding Officer, U.S. Army Signal Research & Development Laboratory, Fort Monmouth, New Jersey, ATTN: ARDC Liaison Office
55	President, U.S. Army Signal Board, Fort Monmouth, New Jersey
56-58	Commanding Officer, U.S. Army Signal Research & Development Laboratory, Fort Monmouth, New Jersey, ATTN: Chief, Security Division (for retransmittal to BJSM)

Copy No.	
59-66	Commanding Officer, U.S. Army Signal Research & Development Laboratory, Fort Monmouth, New Jersey. ATTN: 1 Copy - Director of Research 1 Copy - Technical Documents Center - ADT/E 1 Copy - Chief, Systems Branch, Countermeasures Division 1 Copy - Chief, Detection & Location Branch, Countermeasures Division 1 Copy - Chief, Jamming & Deception Branch, Countermeasures Division 1 Copy - File Unit No. 4, Mail & Records, Countermeasures Division 1 Copy - Chief, Vulnerability Branch, Signal Facilities Division 1 Copy - Reports Distribution Unit, Countermeasures Div. -File
67-74	Commanding Officer, U.S. Army Signal Research & Development Laboratory, Fort Monmouth, New Jersey, ATTN: Reports Distribution Unit (for retransmittal)
75-76	Commanding Officer, U.S. Army Signal Missile Support Agency, White Sands Missile Range, New Mexico, ATTN: SIGWS-EW and SIGWS-FC
77	Commanding Officer, U.S. Naval Air Development Center, Johnsville, Pennsylvania, ATTN: Naval Air Development Center Library
78	Dr. H. W. Farris, Director, Electronic Defense Group, University of Michigan Research Institute, Ann Arbor, Michigan
79-99	Electronic Defense Group Project File, University of Michigan Research Institue, Ann Arbor, Michigan
100	Project File, University of Michigan Research Institute, Ann Arbor, Michigan

Above distribution is effected by Countermeasures Division, Surveillance Dept., USASRDL, Evans Area, Belmar, New Jersey. For further information contact Mr. I. O. Myers, Senior Scientist, telephone PRospect 5-3000, Ext. 61252.